Research Article

Received: 11 September 2015 Revised: 6 November 2015 Accepted article published: 13 November 2015 Published online in Wiley Online Library: 23 December 2015

(wileyonlinelibrary.com) DOI 10.1002/jctb.4848

Photocatalytic degradation of the herbicide clopyralid: kinetics, degradation pathways and ecotoxicity evaluation

Chrysanthi Berberidou,[a†] Vasiliki Kitsiou,[a†] Sofia Karahanidou,[a] Dimitra A Lambropoulou,[a] Athanasios Kouras,[a] Christina I Kosma,[b] Triantafyllos A Albanis[b] and Ioannis Poulios[a*]

Abstract

BACKGROUND: Photocatalytic decomposition and mineralization of the herbicide clopyralid in aqueous solutions has been studied, aiming at an extended kinetic analysis, the elucidation of potential degradation pathways and the determination of ecotoxicity.

RESULTS: The pseudo-first-order degradation kinetics was studied under different operational conditions, such as type of photocatalyst, catalyst loading, initial pH and hydrogen peroxide (H_2O_2) concentration. The degradation rates proved to be strongly influenced by these parameters. Organic chlorine and nitrogen were easily converted into inorganic in the presence of TiO_2 P25, resulting in 90% conversion in both cases within 180 min of illumination, while conversion was enhanced in the presence of H_2O_2. Ten possible transformation products were identified by means of LC-DAD-ESI/MS analysis. Acute toxicity profiles using marine bacteria *Vibrio fischeri* showed an increasing trend during the first 60 min of illumination, which thereafter, progressively decreased.

CONCLUSIONS: Intermediates were formed mainly through pyridine ring transformation, dechlorination and decarboxylation reactions. The increasing trend in ecotoxicity at the first stages of degradation could be attributed to the progressive formation of intermediates more toxic than the parent molecule, or due to synergistic effects among the transformation products.

Keywords: clopyralid; pesticide; photocatalytic; TiO_2; toxicity; intermediates

INTRODUCTION

Introduction of synthetic organic chemicals in agricultural processes during the second half of the twentieth century not only boosted the ability to counter crop-spoiling organisms, but also enabled the control of parasite-borne health and life-threatening diseases (i.e. malaria), improving the quality of life of large populations and allowing better utilization of agricultural areas. However, the widespread use of pesticides has led to widespread contamination of the environment with these bio-recalcitrant organic compounds.[1,2] In highly industrialized countries the problem of pesticide wastes is mainly related to wastewater, recycling, elimination of packaging (containers, etc.) after use and the remediation of contaminated soils. For developing countries, the main problem is the elimination of unused (forbidden), obsolete and unusable pesticide stocks.[1] The United Nations estimates that less than 1% of all pesticides used in agriculture actually reaches the crops. The remainder contaminates the land, the air and particularly the water. These xenobiotics are in many cases toxic and non-biodegradable, with the potential to cause adverse acute or chronic toxic health effects to non-target organisms[1] and to accumulate in the environment through the global trophic network with unpredictable consequences.[3–6]

Clopyralid (3,6-dichloro-2-pyridine-carboxylic acid) is a systemic herbicide from the chemical class of pyridine compounds, often detected in drinking water.[7] It is used to control annual and perennial broadleaf weeds in certain crops and turf and provides control of some brush species on rangeland and pastures. Clopyralid may be persistent in soil under anaerobic conditions and with low microorganism content, with half-life ranging from 15 to more than 280 days.[8] It presents high solubility in water and is particularly stable against hydrolysis and photolysis. Its chemical stability, along with its mobility, enables this herbicide to penetrate through soil, causing long term contamination of ground and surface water supplies[9,10] along with losses in production of certain plant species

* *Correspondence to: Ioannis Poulios, Department of Chemistry, Aristotle University of Thessaloniki, 54124, Thessaloniki, Greece. E-mail: poulios@chem.auth.gr*

† *Equally contributing authors*

a *Department of Chemistry, Aristotle University of Thessaloniki, 54124, Thessaloniki, Greece*

b *Department of Chemistry, University of Ioannina, 45110, Ioannina, Greece*

(i.e. potato crops).[11] Clopyralid is hazardous to certain endangered plant species, beneficial insects[12] and toxic to certain mammals.[13]

Heterogeneous photocatalytic oxidation (TiO_2/UV-A) has been proven to be effective for the degradation of a variety of toxic agrochemical substances, such as insecticides and pesticides, in the presence of artificial or solar illumination, while studies dealing with real or simulated wastewater have revealed that their complete or partial degradation is possible via the above mentioned methods.[14–16] Previous studies have published data on the photocatalytic degradation of clopyralid.[17–19] Our work investigates the photocatalytic decomposition and mineralization of clopyralid employing for the first time a wide range of commercial photocatalysts, providing a thorough kinetic analysis in terms of degradation and mineralization. New intermediates have been identified and detailed degradation pathways have been proposed.[17] Furthermore, for the first time we provide data on the reduction of ecotoxicity based on *Vibrio fischeri* marine bacteria in aqueous solutions of clopyralid treated with TiO_2 P25. The present study is implemented within the framework of a research project aiming at the development of a combined system for the detoxification and reuse of wastewater containing pesticides by solar photocatalysis and constructed wetlands.

MATERIALS AND METHODS

Materials

Clopyralid (3,6-dichloro-2-pyridine-carboxylic acid, CAS No. 1702-17-6, M_r: 192 g mol^{-1}, Product No: 36758, Pestanal, analytical standard) was a product of Fluka (Sigma–Aldrich Laborchemicalien GmbH) and was used as received.

The catalysts used were TiO_2 P25 (Degussa Evonik GmbH, anatase/rutile = 3.6/1, Brunauer-Emmett-Teller (BET) surface area: 50 m^2 g^{-1}, nonporous), TiO_2 UV-100 (Hombikat, 100% anatase, BET: 300 m^2 g^{-1}), TiO_2 Kronos (7000, 7001, 7500, Kronos Worldwide, Inc, 100% anatase, BET: 250 m^2 g^{-1}) and ZnO (Merck, BET: 10 m^2 g^{-1}). All other reagent-grade chemicals were purchased from Merck and were used without further purification. Doubly deionized water was used throughout the study.

Photocatalytic experiments

Experiments were performed in a closed Pyrex cell of 600 mL capacity, fitted with a central 9 W lamp, under magnetic stirring. The cell had inlet and outlet ports for bubbling CO_2 free air during photocatalysis. The spectral response of the irradiation source (Osram Dulux S, 9 W/78) ranged between 350 and 400 nm with a maximum at 366 nm. The incident photon flow of the irradiation source, determined by chemical actinometry using potassium ferrioxalate,[20] was 97×10^{-6} Einstein L^{-1} min^{-1}.

Photocatalysis was conducted at a working volume of 500 mL, at 4.7 ± 0.1 initial pH and constant temperature (25 ± 0.1 °C). Maximum dark adsorption of clopyralid onto the semiconductor surface was achieved within 30 min. At specific time intervals samples of 6 mL were taken and filtered through a 0.45 μm filter (Schleicher and Schuell).

Analytical procedures

Changes in the concentration of clopyralid were monitored via its characteristic absorption band at 280 nm using a UV-Visible spectrophotometer (UV-1700, PharmaSpec, Shimadzu). Since a linear dependence between the initial concentration of the pesticide and the absorption at 280 nm is observed, the photodecomposition was monitored spectrophotometrically at this wavelength.

Determination of dissolved organic carbon (DOC) was conducted according to standard methods by a total organic carbon (TOC) analyser (Shimandzu V_{CSH} 5000).

Inorganic ions were determined in a Shimadzu system consisting of a LC-10 AD pump, a CDD-6A conductometric detector (0.25 μL flow-cell) and a CTO-10A column oven. Cations were separated on an Alltech Universal column (100 mm × 4.6 mm) preceded by a guard column (7.5 mm × 4.6 mm) of the same material using 3 mmol L^{-1} methanesulfonic acid at 1.5 mL min^{-1} constant flow. Anions were separated on an Alltech Allsep column (100 mm × 4.6 mm) preceded by a guard column (7.5 mm × 4.6 mm) of the same material using a phthalic acid and lithium hydroxide mixture of 4 mmol L^{-1} (pH 4.00) at 1.5 mL min^{-1} constant flow. Column and conductivity cell temperatures were held constant at 35 °C and 38 °C, respectively. Mobile phases were degassed with helium stream prior to liquid chromatography (LC). Calibration curves (0.01–10 mg L^{-1}) were constructed for each ion. The method detection limits were 0.03 mg L^{-1} for NH_4^+ and 0.03, 0.07, 0.06 mg L^{-1} for NO_3^-, SO_4^{2-} and Cl^-, respectively.

Some photocatalytic experiments were repeated three times to check the reproducibility of the experimental results. The accuracy of the optical density values was within ± 5%, while in the case of DOC and inorganic ions analysis it was ± 10%.

Liquid chromatography, with diode array detection and electrospray ionisation mass spectrometry (LC DAD ESI/MS) was conducted as follows: the HPLC system consisted of a SIL 20A autosampler and a LC-20AB pump, both from Shimadzu (Kyoto, Japan). The analytes were separated using a C_{18} (Restek) analytical column of 150 × 4.6 mm with 5 μm particle size (Restek, USA). Detection was carried out using a SPD 20A DAD detector coupled in series with the LC-MS 2010EV mass selective detector, equipped with an atmospheric pressure electrospray ionization (ESI) source. The samples were analysed using the ESI interface in positive ionization (PI) mode. For the analysis in PI mode a gradient elution was performed by a binary gradient, composed of solvent A (water/0.1% HCOOH) and solvent B (methanol/0.1% HCOOH) according to the following program: initial conditions 80% A, kept constant for 1 min, decreased to 50% in 4 min, decreased to 10% in 50 min, kept constant for 6 min, returned to the initial conditions after 2 min. Re-equilibration time was set at 2 min, while the total run analysis lasted 60 min. Column temperature was set at 40 °C and the flow rate was 0.2 mL min^{-1}. The drying gas was operated at 10 L min^{-1} flow at 200 °C. The nebulizing pressure was 100 psi, capillary voltage was 4500 V and the fragmentation voltage was set at 5 V (for PI ionization).

Quality assurance and quality control for LC-DAD-ESI/MS analysis

Identification and confirmation of clopyralid in water samples was made by comparing the retention time, identifying the target and qualifier ions and determining the qualifier-to-target ratios of the peak in the samples with that of a pesticide standard. Acceptance criteria for positive identification consisted of retention times within 0.20 min of the expected value and % qualifier-to-target ratios within 30% of the standard (10 mg L^{-1}).

Internal quality control was applied in every batch of samples in order to check if the system is under control. A quality control sample (10 mg L^{-1} standard) was run every five injections, followed by a blank sample (pure methanol). Nine gradients of standard solutions (0.1, 0.5, 1, 5, 10, 25, 50, 75, 100 mg L^{-1}) were adopted. To avoid the impact of linearity issues on quantification accuracy, the target compound concentrations always fall within the middle

range of the standard curve. Calibration curves for the analyte were drawn with five points and the determination coefficients (R^2) of the regression curves were >0.993.

Precision of the LC-MS chromatographic method, determined as relative standard deviation (RSD), was obtained from repeated injections (n = 5) of a sample during the same day (repeatability) and in different days (reproducibility). In all cases RSD% values <10% were obtained.

Limit of detection (LOD) and limit of quantification (LOQ) were defined to be the lowest observable concentration of analyte in spiked water samples giving a signal to-noise (S/N) ratio of 3 and 10, respectively. LOD and LOQ values were 0.020 mg L^{-1} and 0.060 mg L^{-1}, respectively.

Toxicity analysis

Bioluminescence ecotoxicity test using marine bacteria *Vibrio fischeri* was applied to provide information on acute toxicity of the intermediates formed during photocatalysis. The osmolality of the samples was adjusted by 2% w/v NaCl, while pH was adjusted between 6.5 and 8.5. Toxicity was evaluated using the Microtox Model 500 Analyzer (Azur Environmental). Freeze-dried bacteria, reconstitution solution, diluent (2% w/v NaCl) and adjustment solution (non-toxic 22% w/v NaCl) were obtained from Azur. Samples were tested in a medium containing 2% w/v NaCl, in five dilutions and luminescence was recorded after 5, 15 and 30 min incubation. The inhibition of bioluminescence, compared with a toxic-free control to give the percentage of inhibition, was calculated using the Microtox calculation software.

RESULTS AND DISCUSSION

Heterogenous photocatalytic experiments

Results of the degradation of a 40 mg L^{-1} clopyralid solution containing 0.5 g L^{-1} TiO_2 P25, TiO_2 UV-100, ZnO, TiO_2 Kronos 7000, Kronos 7001 and Kronos 7500 under UV-A irradiation are shown in Fig. 1 while the respective initial degradation rates are presented in Table 1. The concentration of clopyralid is plotted as a function of the irradiation time. Under the given experimental conditions, ZnO and TiO_2 P25 in the presence of UV-A appear to be the best catalysts resulting after 180 min of illumination in 95 and 75% degradation of the pesticide, respectively. Although ZnO has similar band gab energy and band edge positions to TiO_2, its non-stoichiometry leads to electron mobility of at least two orders of magnitude higher than TiO_2. This results in a quicker charge transfer with the various species in solution and consequently to lower recombination rates in comparison with TiO_2.[21,22] However, even though ZnO exhibited the highest catalytic efficiency under the studied conditions, its application in photocatalysis is limited due to corrosion and photocorrosion phenomena. At pH values below 9.0 ZnO dissolution takes place, which increases with illumination, as a result of the attack of the Zn–O bonds by the photogenerated holes.[23] This leads to release of Zn^{2+} into the suspension, increasing toxicity, taking into account that for *V. fischeri* the EC_{50} for Zn^{2+} is 1.62 mg L^{-1}.[14,24]

On the other hand, the efficiency of the other commercial forms of TiO_2 in the oxidation of clopyralid under UV-A irradiation is a considerably slower process and decreases in the order: TiO_2 UV-100 < TiO_2 Kronos 7500 ≈ TiO_2 Kronos 7001 < TiO_2 Kronos 7000, with TiO_2 UV-100 resulting in 62% degradation after 180 min of illumination (Fig. 1). The superiority of TiO_2 P25 may be attributed to the morphology of its crystallites, which has been proposed as one of the most critical properties for the photocatalytic efficiency of P25 among various grades of TiO_2. In the case of TiO_2 P25 a transfer of the photogenerated electrons from rutile to anatase particles takes place, leading to stabilization of charge separation and therefore, limits the recombination of the photogenerated carriers.[25] In addition, the small size of rutile particles in this formulation and their close proximity to anatase particles are crucial to enhance the catalyst activity.

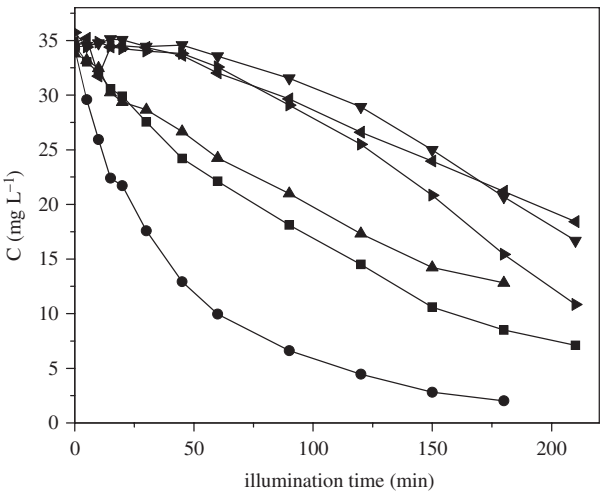

Figure 1. Photocatalytic degradation of 40 mg L^{-1} of clopyralid in the presence of various commercial catalysts at an initial concentration of 0.5 g L^{-1} and UV-A irradiation: (■) TiO_2 P25, (●) ZnO, (▲) TiO_2 UV-100 (▼) TiO_2 Kronos 7000, (◀) TiO_2 Kronos 7001, (▶) TiO_2 Kronos 7500. Error: 5%.

Table 1. Initial rates of photodegradation (r_0) of 40 mg L^{-1} clopyralid in the presence of 0.5 g L^{-1} of various photocatalysts

Conditions	r_0 (mg L^{-1} min^{-1}) ± standard error
TiO_2 P25	0.228 ± 0.009
ZnO	0.828 ± 0.056
TiO_2 UV 100	0.160 ± 0.018
TiO_2 Kronos 7000	0.075 ± 0.004
TiO_2 Kronos 7001	0.087 ± 0.004
TiO_2 Kronos 7500	0.086 ± 0.009

The effect of the initial equilibrium concentration of clopyralid on the initial reaction rate (r_o) of photodecomposition is shown in Fig. 2. The r_o values were independently obtained by a linear fit of the C–t data in the range 5–50 mg L^{-1} of initial clopyralid concentration. The curve is reminiscent of a Langmuir type isotherm, for which the rate value of photodecomposition first increases and then reaches a saturation value at higher concentrations of clopyralid.

The influence of the initial concentration of an organic compound on the photocatalytic degradation rate of most organic compounds is described by a pseudo-first-order kinetics, which is rationalized in terms of the Langmuir–Hinshelwood model, modified to be valid for reactions occurring at a solid–liquid interface:[26,27]

$$r_0 = -\frac{dC}{dt} = \frac{k_r KC}{1 + KC} \quad (1)$$

where r_o is the initial degradation rate and C is the concentration of the organic substrate. K represents the equilibrium constant

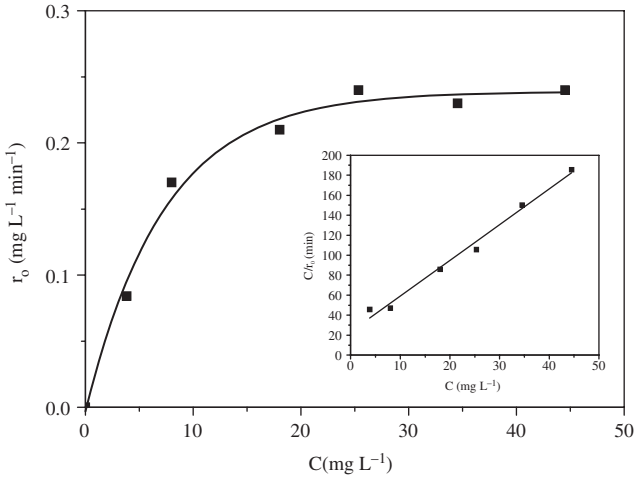

Figure 2. Plot of r_0 vs C at various initial concentrations of clopyralid from 5 to 50 mg L^{-1} for constant concentration of TiO_2 P25 at 0.5 g L^{-1}. Inset: linear transformation of C/r_0 vs C according to Equation (2).

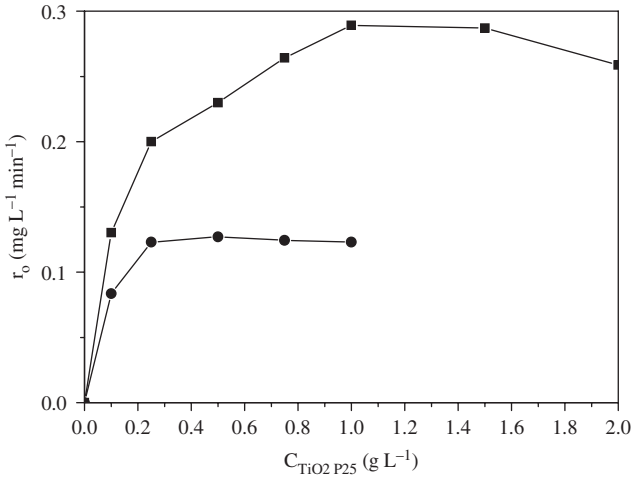

Figure 3. Effect of the TiO_2 P25 concentration on initial (■) degradation (r_0) and (●) mineralization (r_{DOC}) rates of clopyralid, during heterogenous photocatalysis under UV-A irradiation for 40 mg L^{-1} of the pesticide.

for adsorption of the organic substrate onto the semiconductor and k_r reflects the limiting rate constant of reaction at maximum coverage under the given experimental conditions. This equation can be used when data demonstrate linearity plotted as follows:

$$\frac{C}{r_0} = \frac{1}{k_r K} + \frac{C}{k_r} \qquad (2)$$

As indicated in the inset of Fig. 2 the plot of the reciprocal initial rate, r_0, as a function of the initial concentration, C, yields for constant concentration of TiO_2 P25 at 0.5 g L^{-1} a straight line. The k_r and K values calculated according to Equation (2) from the slope and the intercept with the $1/r_o$ axis of the resulting straight line ($R^2 = 0.98$), were 0.28 ± 0.01 mg L^{-1} min^{-1} ($1.46\ 10^{-6} \pm 0.05\ 10^{-9}$ mol L^{-1} min^{-1}) and 0.15 ± 0.03 L mg^{-1} (0.78 ± 0.16 L mol^{-1}), respectively.

TiO_2 dosage in slurry photocatalytic processes is an important factor that can strongly influence the degradation of the organic compound. The optimum quantity depends on the nature of the organic compound, as well as on the photoreactor's geometry. The values of the initial degradation rate in relation to the catalyst dose follow a Langmuir type isotherm, suggesting that r_0 might reach a saturation value at higher TiO_2 concentrations.[28] In this study, the optimum value for TiO_2 P25 is 1.0 g L^{-1}, while further increase in the amount of TiO_2 leads to a slight decrease in the efficiency of photodegradation (Fig. 3). This limit depends on the geometry and the working conditions of the reactor and corresponds to the optimum of light absorption. Above this optimum concentration, the suspended particles of the catalysts block the UV-light passage and increase the light scattering. Furthermore, the decrease of the reaction rate at high catalyst concentrations is due to other phenomena such as agglomeration (particle–particle interactions), resulting in a loss of surface area available for light-harvesting.[29] On the contrary, the increase of TiO_2 P25 loading leads to no further increase of the initial mineralization rate at concentrations above 0.25 g L^{-1} (Fig. 3).

The pH value, on the other hand, plays an important role in the photocatalytic degradation of various organic pollutants. Some properties of the photocatalyst, such as surface charge state and flat band potential are highly pH dependent, while electrostatic attraction or repulsion between the catalyst's surface and the

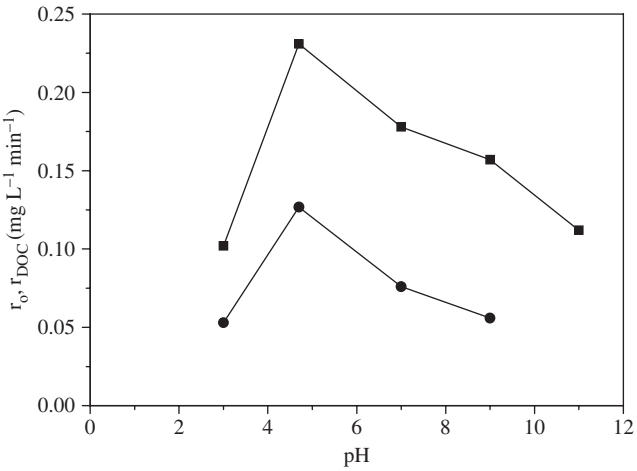

Figure 4. Effect of pH on clopyralid initial degradation and mineralization rates during heterogeneous photocatalytic oxidation of 40 mg L^{-1} of clopyralid in the presence of 0.5 g L^{-1} TiO_2 P25 and UV-A irradiation: (■) r_o,(●) r_{DOC}.

organic molecule, depending on the ionic form of the organic compound (anionic or cationic) enhances or inhibits, respectively, the photodegradation rate.[30–32] Moreover, pH influences the size of TiO_2 aggregates, the interaction of the solvent molecules with the catalyst and the type of radicals or intermediates formed during the photocatalytic process. All of these factors have a significant influence on the adsorption of organic molecules onto TiO_2 and affect the observed removal rates.[19] The effect of pH on clopyralid initial degradation and mineralization rates has been studied and the results are displayed in Fig. 4. As the pH increases from 3.0 to 4.7 (natural pH), the initial degradation and mineralization rates, also increase by a factor of approximately 2.5 in both cases, rendering 4.7 the most favorable pH value for decomposition of the herbicide. However, both degradation and mineralization rates gradually decrease as photocatalysis takes place in neutral or progressively higher alkaline pH values. Clopyralid is a weak acid having pKa values of 1.4 and 4.4.[8] Since TiO_2 has a zero point of charge (zpc) of approximately 6.35, the surface of TiO_2 is positively charged ($TiOH^+$) in solutions with a pH lower

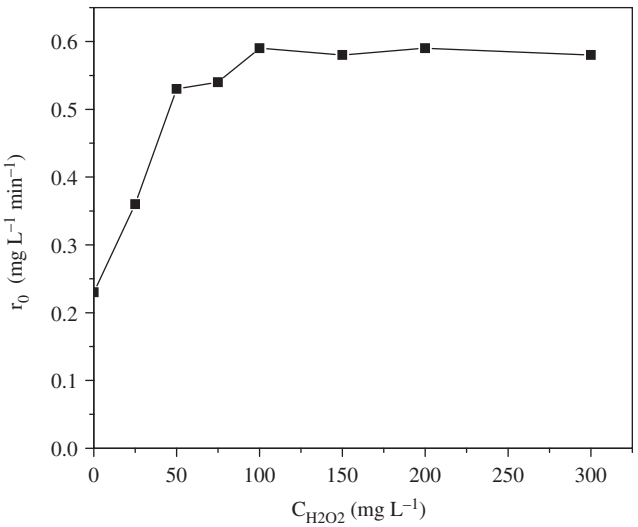

Figure 5. Effect of H_2O_2 concentration in the initial degradation rate of 40 mg L^{-1} of clopyralid in the presence of 0.5 g L^{-1} TiO_2 P25 and UV-A.

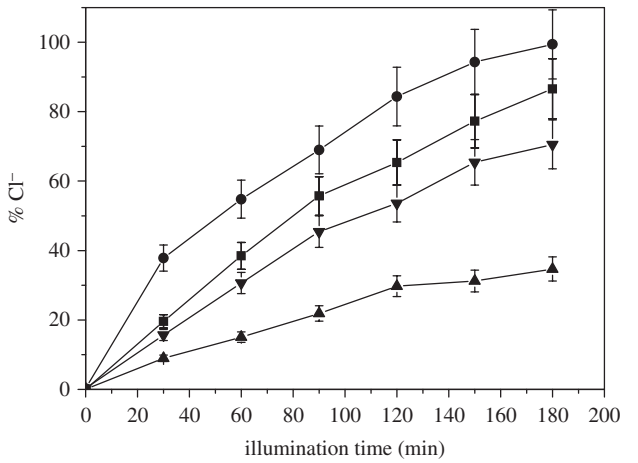

Figure 6. Release of chloride ions during the mineralization of 40 mg L^{-1} clopyralid in the presence of 0.5 g L^{-1} catalyst and UV-A irradiation: (■) TiO_2 P25, (●) TiO_2 P25 and 100 mg L^{-1} H_2O_2, (▲) TiO_2 UV-100, (▼) TiO_2 UV-100 and 100 mg L^{-1} H_2O_2.

than 6.35, favorable for attracting anions, and TiO_2 deprotonates in solutions with a pH higher than 6.35, hence its surface becomes negatively charged (TiO^-), favorable for repelling anions.[33] At pH 3.0, clopyralid ionizes significantly to cations and the surface charges of TiO_2 are predominantly positive ($pH < pzc_{TiO2}$). This creates an unfavorable condition for attracting clopyralid to the surface of TiO_2, resulting in low degradation rates. As pH increases from 3.0 to 4.7 clopyralid becomes less positively charged and at pH 4.7 is even negatively charged, yet TiO_2 surface is still positively charged, favorable for attraction of the two species and for high degradation and mineralization rates (Fig. 4). A further increase of pH, in particular beyond pzc_{TiO2} (6.35), results in accumulation of negative charges on the surface of TiO_2, causing repulsion of the negatively charged clopyralid molecules. Thus, surface adsorption and initial degradation and mineralization rates decrease. Similar results on the effect of pH on the initial degradation rate of clopyralid were reported by C. Tizaoui *et al.*[19]

The addition of species with the potential to capture the photogenerated electrons, such as hydrogen peroxide and potassium peroxydisulfate, to TiO_2/UV-A suspensions is an extensively studied procedure often leading to an acceleration of the photocatalytic degradation rate.[14,34] In our case the photocatalytic oxidation of 40 mg L^{-1} of clopyralid in the presence of 0.5 g L^{-1} TiO_2 P-25 has been studied at different initial H_2O_2 concentrations (Fig. 5). The reaction kinetics were similar to those observed without the oxidants. Photocatalytic efficiency increases as the concentration of H_2O_2 rises, reaching an optimum at 100 mg L^{-1}. Consequently, it reaches a plateau at peroxide concentrations between 150 and 300 mg L^{-1}. The presence of H_2O_2 at an initial pH value of 4.7 ± 0.1, and at concentrations in the range 100–300 mg L^{-1} increases the initial reaction rate almost by a factor of 2, in comparison to the one in the absence of H_2O_2.

Degradation by-products and reaction pathways

Photocatalytic mineralization of clopyralid proceeds through the formation of various reaction intermediates, whose carbon atoms are eventually converted to carbon dioxide, while heteroatoms are converted to inorganic ions that remain in the liquid phase. Clopyralid mineralization can be described by the following overall reaction scheme:

$$C_6H_3O_2NCl_2 + 13/2\ O_2 \rightarrow 6CO_2 + HNO_3 + 2HCl \qquad (3)$$

To elucidate the routes through which clopyralid is converted to reaction by-products and eventually to end-products, besides the DOC reduction (Figs 3 and 4), samples were analyzed with respect to: (i) the release of inorganic chlorine and nitrogen species in the reaction mixture; and (ii) the identification of major intermediates.

Figures 6 and 7 show temporal profiles of chloride anions and total inorganic nitrogen (i.e. contained in nitrates, nitrites and ammonium ions), respectively, released during the photocatalytic oxidation of clopyralid. Profiles do not show actual concentrations but they correspond to the percentage of the theoretical amount of chloride or nitrogen initially present in the clopyralid molecule. Organic chlorine is easily converted into inorganic in the presence of TiO_2 P25 (almost 87% conversion within 180 min of illumination, Fig. 6). TiO_2 UV-100, under the same experimental conditions, leads to 35% conversion of chlorine, while in both cases the photocatalyst's activity is enhanced in the presence of H_2O_2.

Similar results are obtained regarding the conversion of nitrogen of the pyridine ring of clopyralid in NO_3^- and NH_4^+. Figure 7 shows concentration–time profiles of total inorganic nitrogen (i.e. the sum of nitrogen contained in NO_3^-, NH_4^+ and NO_2^-) as a percentage of the theoretical nitrogen in clopyralid, under various experimental conditions. In all cases, ammonium and nitrate were the dominant inorganic species formed during photocatalytic degradation, while only trace amounts of NO_2^- were detected which, upon prolonged irradiation, were oxidized to NO_3^-. Nitrogen conversion is more effective in the presence of TiO_2 P25 compared with TiO_2 UV-100 (almost 80% and 30% conversion rates, respectively, after 180 min of illumination), while in both cases the activity of the catalysts is enhanced in the presence of H_2O_2.

The transformation mechanism of clopyralid during the photocatalytic process was investigated. Ten (10) transformation products (TPs) were identified on the basis of molecular ions and mass fragment ions by MS spectrum during photocatalysis in the presence of 0.5 g L^{-1} TiO_2 P25 and UV-A. Information concerning the TPs is summarized in Table 2, while Fig. 8 shows the tentative transformation pathways of clopyralid, the products detected and the hypothetical intermediates within bracket (blue color). It has

Table 2. LC-MS data of clopyralid and its detected transformation products during heterogenous photocatalysis in the presence of 0.5 g L^{-1} TiO_2 P25 and UV-A irradiation

TPs	t_R (min)	Elemental composition	Molecular ion (*m/z*)	Mass fragments(*m/z*) (% abundance)
TP190	10.1	C_6 H_4 Cl NO_4	190	107(84.82), 110(20.24), 134(23.41), 146(23.24), 158(30.26), 162(24.30), 174.00(41.87), 190(100.00)
TP174A	11.2	C_6 H_4 Cl NO_3	174	110(9.03), 134(14.25), 158(13.20), 162(10.92), 174(100.00)
TP174B	12.4	C_6 H_4 Cl NO_3	174	107(20.28), 134(21.71), 158(31.35), 162(22.78), 174(100.00)
TP130A	20.2	C_5 H_4 Cl NO	130	79(28.27), 97(15.42), 130(100.00)
TP130B	21.4	C_5 H_4 Cl NO	130	79(28.27), 97(15.42), 130(100.00)
TP208A	25.7	C_6 H_4 O_3 N Cl_2	208	107(20.65), 134(22.76), 162(23.75), 174(100.00), 190(28.37), 208(51.19)
TP208B	28.4	C_6 H_4 O_3 N Cl_2	208	107(16.46), 134(18.81), 162(18.77), 174(77.58), 190(25.10), 208(100.00)
Clopyralid	29.6	C_6 H_4 O_2 N Cl_2	192	110(3.82), 146(4.84), 164(6.67), 174(11.04), 192(100.00), 208(9.97), 220(4.42), 256(4.41), 291(4.37), 319(4.53), 337(5.68), 338(4.58)
TP164	34.8	C_5 H_4 O N Cl_2	164	110(9.17), 146(10.84), 164(100.00)
TP220	48.7	-	220	110(17.17), 134(24.17), 162(24.13), 174(63.74), 192(27.17), 208(29.55), 220(100.00)
TP337	51.21	C_{11} H_4 Cl_4 N_2 O_2	337	158(37.02), 220(60.11), 256(100.00), 291(46.17), 319(47.90), 337(71.76), 338(46.83)

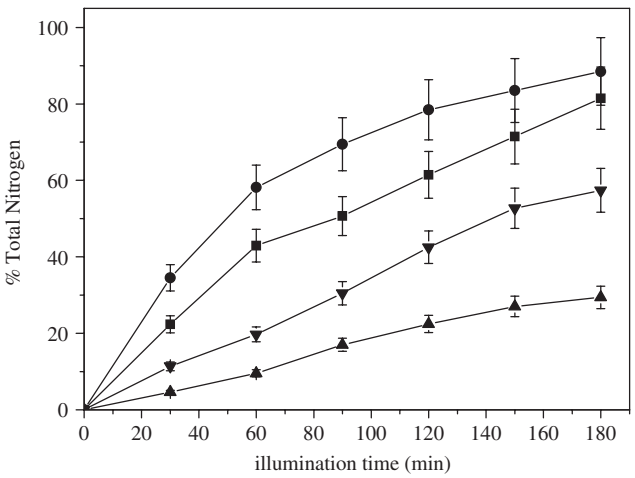

Figure 7. Release of total inorganic nitrogen during photocatalytic mineralization of 40 mg L^{-1} clopyralid, in the presence of 0.5 g L^{-1} catalyst and UV-A irradiation: (■) TiO_2 P25, (●) TiO_2 P25 and 100 mg L^{-1} H_2O_2, (▲) TiO_2 UV-100, (▼) TiO_2 UV-100 and 100 mg L^{-1} H_2O_2.

been concluded that degradation of clopyralid is mainly initiated by pyridine ring transformation (Pathway1, P1), dechlorination (Pathway 2, P2) and decarboxylation (Pathway 3, P3). In Pathway 1, TP207A and TP207B are both obtained from the hydroxyl oxidation at meta or para position of the pyridine ring. Further hydroxylation led to decarboxylation and opening of the pyridine ring. Pathway 2 results from the elimination of one chlorine atom by the clopyralid molecule, which leads to the formation of the two hydroxyl isomers, namely 6-chloro-3-hydroxypicolinic acid (TP174A) and 3-chloro-6-hydroxypicolinic acid (TP174B). Afterwards, these products undergo a series of hydroxylation and oxidation processes that substitute the next chlorine atom of the aromatic ring and generate the corresponding phenolic and keto products. The oxidative ring-opening reactions follow, to form the short-chain carboxylic acids and inorganic ions. In the third pathway, the parent molecule, upon the transfer of one electron can form a radical anion, which after decarboxylation and attack of the OH• leads to the formation of 3,6-dichloropyridin-2-ol (TP164). Successive •OH radical attack at halogenated and non-halogenated sites leads, ultimately, to hydroxy derivatives and/or keto intermediates and finally, to open-ring products. Finally, the last pathway involves the formation of the dimer derivative (3,3′,6,6′-tetrachloro-2,4′-bipyridine-2′-carboxylic acid, TP337), through the reaction of the intermediate radical species.

The reaction pathways proposed here, although with some similarities, differ from others previously reported in the literature. It has been reported that in electro-Fenton processes, clopyralid degradation occurs mainly due to the initial dechlorination and formation of hydroxy derivatives by the electrophilic substitution of the chlorine atoms in which the hydroxyl radicals causes an ipso-attack on C-carrying.[35] In the TiO_2 photocatalytic treatment reported by Šojić *et al.*,[17] clopyralid showed similar, but not identical, reaction pathways with our study, leading to hydroxylated and decarboxylated intermediates and dimer products. However, formation of chloro-hydroxypicolinic acid derivatives, 5-chloropyridin-2-ol and 6-chloropyridin-3-ol, was not observed by Šojić *et al.*

For better knowledge of the photocatalytic process and assessment of the main transformation routes, an evaluation of the TPs generated during photocatalysis in the presence of 0.5 g L^{-1} TiO_2 P25 and UV-A was carried out, as a function of the peak area obtained in the LC analysis. Typical bell-shaped profiles were obtained in most cases (Fig. 9). Compounds detected at higher concentration in this period were TP174A and TP164, suggesting that P2 and P3 are among the major pathways in the clopyralid degradation. The monochlorinated products, TP174A and TP174B, appear promptly; they reach a concentration maximum after 10 and 30 min, respectively, before being degraded in turn. By comparing the evolution profiles for these products it appears that the TP174A product at retention time (t_R) 11.2 min is the most abundant, whereas the one at $t_R = 12.4$ min is the least concentrated, indicating differences in ionization efficiency or a partially regioselective attack from the •OH radicals. The same observation applies to TP208 product, with the species at $t_R = 25.7$ min (TP208A) being the most abundant compared with that at $t_R = 28.4$ min (TP208B). After 30 min the concentration of all TP174 and TP208 isomers decreases forming second generation products. The rest of TPs were present at lower concentrations. After a $t_R = 120$ min, most of the TPs were present at low concentrations. These data are in concordance with the fast accumulation rate of chloride ions (Fig. 6) and DOC values measured during the assays (Figs. 3 and 4).

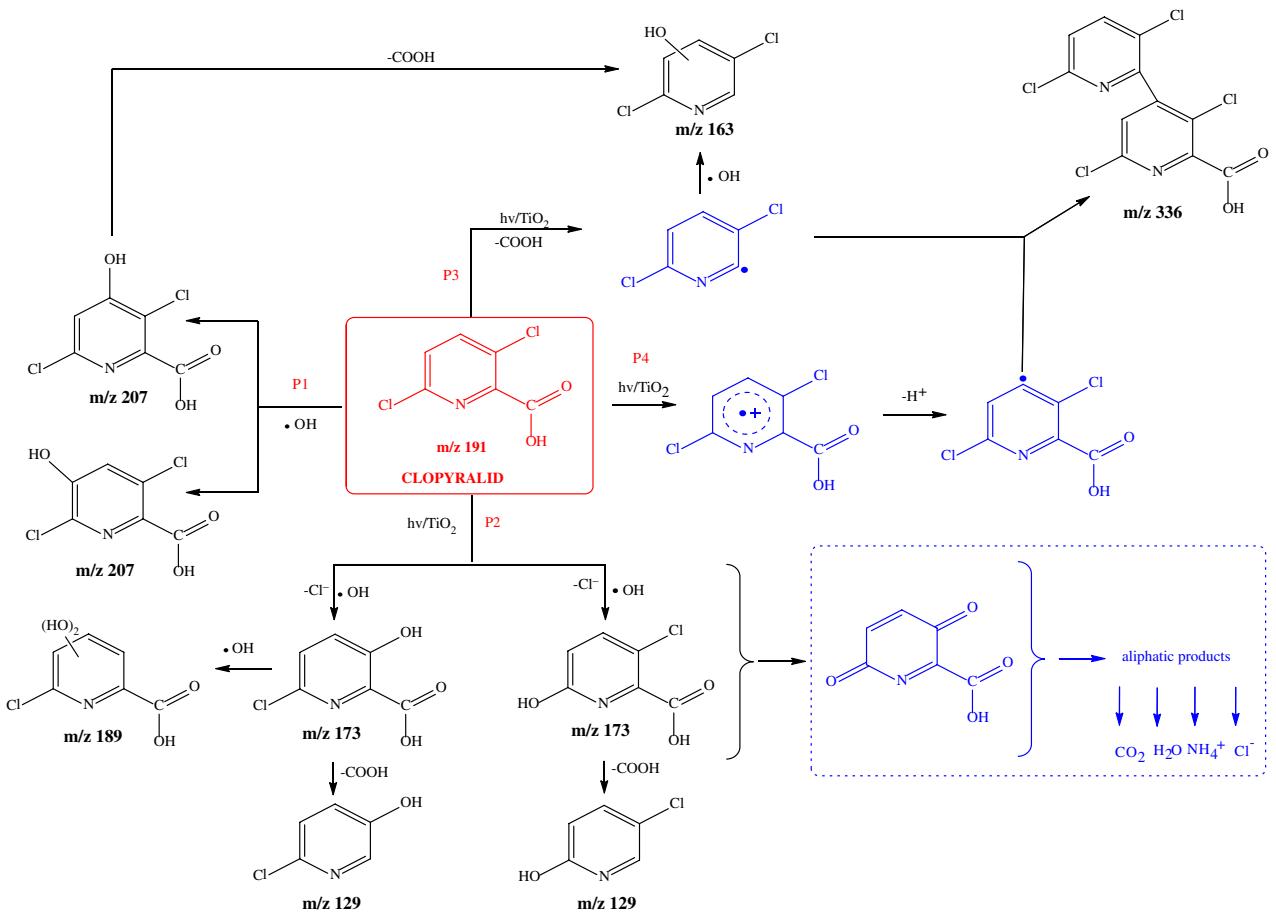

Figure 8. Tentative pathways of TiO_2 transformation of 40 mg L^{-1} clopyralid during heterogenous photocatalysis in the presence of 0.5 g L^{-1} TiO_2 P25 and UV-A irradiation.

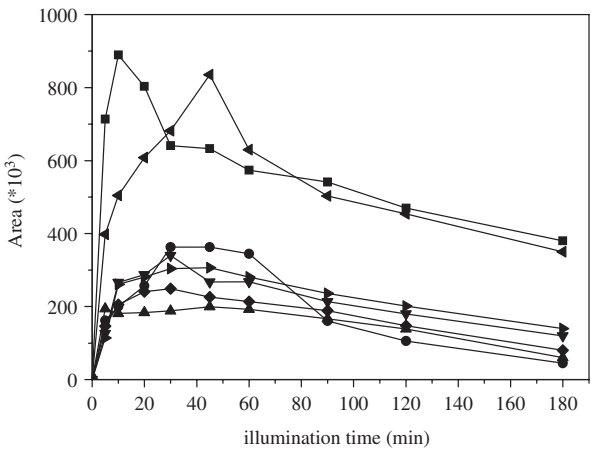

Figure 9. Evolution profile of major transformation products (TPs) during clopyralid degradation in the presence of 0.5 g L^{-1} TiO_2 P25 and UV-A irradiation: (■) TP174A, (●) TP174B, (▲) TP208A, (▼) TP208B, (◀) TP164, (▶) TP220, (◆) TP337.

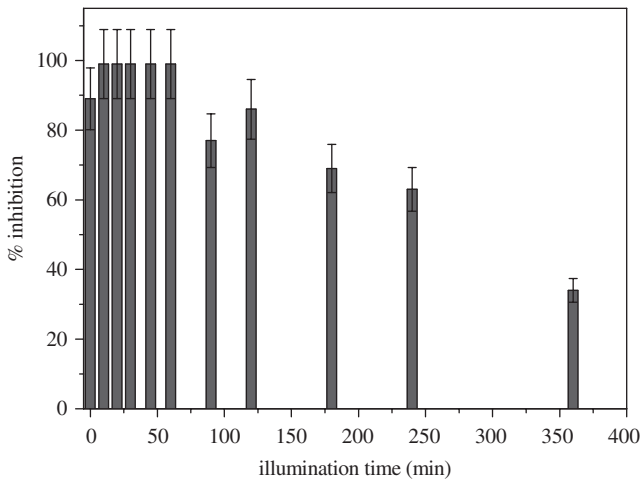

Figure 10. Variation of ecotoxicity of 40 mg L^{-1} clopyralid during photocatalytic oxidation in the presence of 0.5 g L^{-1} TiO_2 P25 and UV-A irradiation.

Acute toxicity evaluation

An important goal of this study was to determine whether or not the TPs generated during the photocatalytic treatment present residual toxicity. Thus, acute toxicity of samples collected at various timepoints during photocatalysis in the presence of 0.5 g L^{-1} TiO_2 P25 and UV-A was evaluated employing *V. fischeri* marine bacteria, by estimating the percentage of inhibition of each sample after 5, 15 and 30 min exposure of the bacteria to the photocatalytically treated samples (Fig. 10).

The untreated clopyralid solution (40 mg L^{-1}) was found to be very toxic to *V. fischeri* inducing an initial inhibition of 83% after 15 min incubation. The toxicity profile of the irradiated

mixtures showed an increasing trend of toxicity which could be attributed to the progressive formation of more toxic compounds than the parent herbicide, or to synergistic effects among the TPs. The highest toxicity (100% inhibition) was observed at irradiation times where the majority of the identified TPs attained almost their maximum concentration, suggesting that clopyralid and its TPs have high acute toxicity effects on the tested bacteria. Bioluminescence inhibition values remained stable at the initial stages of the transformation process between 10 and 60 min. Thereafter, inhibition of bioluminescence was progressively decreased (34% at 360 min), implying that total detoxification would be achieved at prolonged irradiation times. A similar trend in toxicity evaluation was also observed by Solís *et al.*, who studied the TPs of clopyralid after ozonation treatment.[36]

CONCLUSIONS

Heterogenous photocatalytic degradation and mineralization of the herbicide clopyralid has been studied. Degradation follows pseudo-first-order kinetics, with TiO_2 P25 providing the best results among the tested commercial TiO_2. Catalyst's loading, H_2O_2 concentration and pH affect the degradation kinetics. The initial degradation rate sharply increases with increasing TiO_2 P25 loading, especially up to 1.0 g L^{-1}, while addition of 100 mg L^{-1} H_2O_2 achieves maximum increase of the initial degradation rate. The most favorable pH for decomposition of the herbicide was 4.7, while both degradation and mineralization rates gradually decrease as photocatalysis takes place in neutral or alkaline pH values. Organic chlorine and nitrogen is easily converted into inorganic in the presence of 0.5 g L^{-1} TiO_2 P25 presenting almost 90% conversion within 180 min illumination in both cases. Photocatalysis by TiO_2 UV-100/UV-A, under the same experimental conditions, leads to lower conversion rates. In both cases the photocatalyst's activity is enhanced in the presence of H_2O_2.

Degradation of clopyralid was mainly initiated by pyridine ring transformation, dechlorination, and decarboxylation reactions. The toxicity profile of the irradiated samples initially showed an increasing trend possibly due to the formation of toxic intermediates, or due to synergistic effects among them. Thereafter, ecotoxicity decreased implying that total detoxification would be achieved at prolonged irradiation times.

These findings suggest that TiO_2 mediated photocatalysis has the potential to provide a sustainable solution in the detoxification of wastewater containing recalcitrant pesticides, either alone or in combination with other methods, i.e. biological degradation in constructed wetlands, reducing the relevant environmental impact and creating water suitable for reuse applications (e.g. irrigation).

ACKNOWLEDGEMENTS

The study was implemented within the framework of the research project entitled 'A novel method for detoxification and reuse of wastewater containing pesticides by solar photocatalysis and constructed wetlands' (project No: 957) of the Action ARISTEIA of the Operational Program 'Education and Lifelong Learning' (Action's Beneficiary: General Secretariat for Research and Technology) and is co-financed by the European Social Fund (ESF) and the Greek State.

REFERENCES

1 NATO Science for peace and security series - C: Environmental Security-Environmental security assessment and managment of obsolate pesticides in southeast Europe. Springer (11–17 September 2012).
2 Wei L, Shifu C, Wei Z and Sujuan Z, Titanium dioxide mediated photocatalytic degradation of methamidophos in aqueous phase. *J Hazard Mater* **164**:154–160 (2009).
3 Arias-Estevez M, Lopez-Periago E, Martinez-Carballo E, Simal-Gandara J, Mejuto JC and Garcia-Rio L, The mobility and degradation of pesticides in soils and the pollution of groundwater resources. *Agric Ecosyst Environ* **123**:247–260 (2008).
4 Readman JW, Albanis TA, Barcelo D, Galassi S, Tronczynski J and Gabrielides GP, Herbicide contamination of mediterranean estuarine waters - results from a med pol pilot survey. *Mar Pollut Bull* **26**:613–619 (1993).
5 Sharma MVP, Kumari VD and Subrahmanyam M, TiO(2) Supported over SBA-15: an efficient photocatalyst for the pesticide degradation using solar light. *Chemosphere* **73**:1562–1569 (2008).
6 Thurman EM and Meyer MT, Herbicide metabolites in surface water and groundwater: introduction and overview. *ACS Symp Ser* **630**:1–15 (1996).
7 Donald DB, Cessna AJ, Sverko E and Glozier NE, Pesticides in surface drinking-water supplies of the northern Great Plains. *Environ Health Persp* **115**:1183–1191 (2007).
8 Corredor MC, Mellado JMR and Montoya AR, EC(EE) process in the reduction of the herbicide clopyralid on mercury electrodes. *Electrochim Acta* **51**:4302–4308 (2006).
9 Huang XJ, Pedersen T, Fischer M, White R and Young TM, Herbicide runoff along highways. 1. Field observations. *Environ Sci Technol* **38**:3263–3271 (2004).
10 Sakaliene O, Papiernik SK, Koskinen WC, Kavoliunaite I and Brazenaitei J, Using lysimeters to evaluate the relative mobility and plant uptake of four herbicides in a rye production system. *J Agric Food Chem* **57**:1975–1981 (2009).
11 Wall DA, Potato (solanum-tuberosum) response to simulated drift of dicamba, clopyralid and tribenuron. *Weed Sci* **42**:110–114 (1994).
12 Hassan SA, Bigler F, Bogenschutz H, Boller E, Brun J, Calis JNM *et al.*, Results of the 6th joint pesticide testing program of the iobc/wprs working group pesticides and beneficial organisms. *Entomophaga* **39**:107–119 (1994).
13 Hayes WC, Smith FA, John JA and Rao KS, Teratologic evaluation of 3,6-Dichloropicolinic acid in rats and rabbits. *Fundament Appl Toxicol: Official J Soc Toxicol* **4**:91–97 (1984).
14 Kitsiou V, Filippidis N, Mantzavinos D and Pouios I, Heterogeneous and homogeneous photocatalytic degradation of the insecticide imidacloprid in aqueous solutions. *Appl Catal B - Environ* **86**:27–35 (2009).
15 Konstantinou IK and Albanis TA, Photocatalytic transformation of pesticides in aqueous titanium dioxide suspensions using artificial and solar light: intermediates and degradation pathways. *Appl Catal B - Environ* **42**:319–335 (2003).
16 Toepfer B, Gora A and Li Puma G, Photocatalytic oxidation of multicomponent solutions of herbicides: reaction kinetics analysis with explicit photon absorption effects. *Appl Catal B - Environ* **68**:171–180 (2006).
17 Sojic DV, Anderluh VB, Orcic DZ and Abramovic BF, Photodegradation of clopyralid in TiO2 suspensions: identification of intermediates and reaction pathways. *J Hazard Mater* **168**:94–101 (2009).
18 Sojic DV, Despotovic VN, Abazovic ND, Comor MI and Abramovic BF, Photocatalytic degradation of selected herbicides in aqueous suspensions of doped titania under visible light irradiation. *J Hazard Mater* **179**:49–56 (2010).
19 Tizaoui C, Mezughi K and Bickley R, Heterogeneous photocatalytic removal of the herbicide clopyralid and its comparison with UV/H2O2 and ozone oxidation techniques. *Desalination* **273**:197–204 (2011).
20 Braun AM, Maurette MT and Oliveros E, *Photochemical Technology*. Wiley, New York (1991).
21 Baxter JB and Schmuttenmaer CA, Conductivity of ZnO nanowires, nanoparticles, and thin films using time-resolved terahertz spectroscopy. *J Phys Chem B* **110**:25229–25239 (2006).
22 Meulenkamp EA, Electron transport in nanoparticulate ZnO films. *J Phys Chem B* **103**:7831–7838 (1999).

23 Kositzi M, Poulios I, Samara K, Tsatsaroni E and Darakas E, Photocatalytic oxidation of cibacron yellow LS-R. *J Hazard Mater* **146**:680–685 (2007).
24 Kaiser KLE and Palabrica VS, Photobacterium phosphoreum toxicity data index. *Water Qual Res J Canada* **26**:361 (1991).
25 Hurum DC, Agrios AG, Gray KA, Rajh T and Thurnauer MC, Explaining the enhanced photocatalytic activity of Degussa P25 mixed-phase TiO2 using EPR. *J Phys Chem B* **107**:4545–4549 (2003).
26 Alekabi H and Serpone N, Kinetic-studies in heterogeneous photocatalysis .1. photocatalytic degradation of chlorinated phenols in aerated aqueous-solutions over Tio2 supported on a glass matrix. *J Phys Chem - US* **92**:5726–5731 (1988).
27 Cunningham J, Al-Sayyed G and Srijaranai S, Adsorption of model pollutants onto TiO2 particles in relation to photoremediation of contaminated water, in *Aquatic and Surface Photochemistry*, ed by Heltz G, Zepp R and Crosby D. Lewis Publishers, CRC Press, 317–348 (1994).
28 Parra S, Olivero J and Pulgarin C, Relationships between physicochemical properties and photoreactivity of four biorecalcitrant phenylurea herbicides in aqueous TiO2 suspension. *Appl Catal B - Environ* **36**:75–85 (2002).
29 Robert D, Dongui B and Weber JV, Heterogeneous photocatalytic degradation of 3-nitroacetophenone in TiO2 aqueous suspension. *J Photochem Photobiol A* **156**:195–200 (2003).
30 Helali S, Dappozze F, Horikoshi S, Bui TH, Perol N and Guillard C, Kinetics of the photocatalytic degradation of methylamine: influence of pH and UV-A/UV-B radiant fluxes. *J Photochem Photobiol A* **255**:50–57 (2013).
31 Philippidis N, Sotiropoulos S, Efstathiou A and Poulios I, Photoelectrocatalytic degradation of the insecticide imidacloprid using TiO2/Ti electrodes. *J Photochem Photobiol A* **204**:129–136 (2009).
32 Zielinska B, Grzechulska J, Kalenczuk RJ and Morawski AW, The pH influence on photocatalytic decomposition of organic dyes over A11 and P25 titanium dioxide. *Appl Catal B - Environ* **45**:293–300 (2003).
33 Halmann MM, *Photodegradation of Water Pollutants*. CRC Press, Boca Raton (1996).
34 Malato S, Blanco J, Maldonado MI, Fernandez-Ibanez P and Campos A, Optimising solar photocatalytic mineralisation of pesticides by adding inorganic oxidising species; application to the recycling of pesticide containers. *Appl Catal B - Environ* **28**:163–174 (2000).
35 Ozcan A, Oturan N, Sahin Y and Oturan MA, Electro-Fenton treatment of aqueous Clopyralid solutions. *Int J Environ Anal Chem* **90**:478–486 (2010).
36 Solis RR, Rivas FJ, Gimenoa O and Pɪrez-Bote JL, Photocatalytic ozonation of clopyralid, picloram and triclopyr. Kinetics, toxicity and influence of operational parameters. *J Chem Technol Biotechnol* DOI: 10.1002/jctb.4542 (2014).

